1999

An objective method for determining principal time scales of coherent eddy structures using orthonormal wavelets

Jozsef Szilagyi
University of Nebraska - Lincoln, jszilagyi1@unl.edu

Marc B. Parlange
The Johns Hopkins University

Gabriel G. Katul
Duke University

John D. Albertson
University of Virginia

ELSEVIER

PII: S0309-1708(98)00046-3

Advances in Water Resources Vol. 22, No. 6, pp 561–566, 1999

0309-1708/99/$ – see front matter

An objective method for determining principal time scales of coherent eddy structures using orthonormal wavelets

Jozsef Szilagyi[a,*], Marc B. Parlange[b], Gabriel G. Katul[c] & John D. Albertson[d]

[a]*Conservation and Survey Division, Institute of Agriculture and Natural Resources, University of Nebraska-Lincoln, 113 Nebraska Hall, Lincoln, NE 68588-0517, USA*
[b]*Department of Geography and Environmental Engineering, The Johns Hopkins University, Baltimore, MD, 21218-2686, USA*
[c]*School of the Environment, Duke University, Durham, NC 27708-0328, USA*
[d]*Department of Environmental Sciences, University of Virginia, Charlottesville, VA, 22903, USA*

(Received 13 April 1998; accepted 28 October 1998)

A new, parameter-free method, based on orthonormal wavelet expansions is proposed for calculating the principal time scale of coherent structures in atmospheric surface layer measurements. These organized events play an important role in the exchange of heat, mass, and momentum between the land and the atmosphere. This global technique decomposes the energy contribution at each scale into organized and random eddy motion. The method is demonstrated on vertical wind velocity measurements above bare and vegetated surfaces. It is found to give nearly identical results to a local thresholding approach developed for signal de-noising that assigns the wavelet coefficients to organized and random motion. The effect of applying anti- and/or near-symmetrical wavelet basis functions is also investigated. © 1999 Elsevier Science Limited. All rights reserved

1 INTRODUCTION

The important role of coherent structures in the atmospheric boundary layer (ABL) for the exchange of heat, mass, and momentum across the land-atmosphere interface is well established[4,16–18,27,38,40,44]. According to Wilczak's[44] definition, coherent structures are distinct large-scale fluctuation patterns regularly observed in turbulent flows. These patterns or regions of the flow field are spatially and temporally correlated with themselves and statistically significant with respect to the turbulence energy of the flow[41]. When viewed in this way, turbulent flows are comprised of a superposition of organized, coherent structures and disorganized, or "random" background activity[21,43].

Coherent structures in the atmosphere can be so markedly developed that they are clearly identifiable in measured time series as "ramps" arising from the sweep-ejection motion in the surface layer[1,16,17,19,27,36,43]. Gao *et al.*,[16,17] identified coherent structures above a forest canopy having regularly repeated organized cycles of ejection-like upward flow and the subsequent sweep-like descending motions. Shaw *et al.*,[40] identified coherent bursting structures in turbulent shear flows for plant canopies. A large amount (>75%) of the total vertical momentum and heat flux was found to take place in these bursting events.

Wavelet transforms have become an important tool for identifying and studying coherent structures[7,13,15,19,25,26,30–32,43]. These wavelet-based techniques often provide useful information which is advancing our understanding of turbulent transport, for example, the flux of water vapor into the atmosphere[21,23,24].

Wavelet transforms allow the decomposition of data into different frequency or scale components distributed in space[8,28–30,33,34]. Although there are many types of wavelet transforms, they can all be classified as either continuous or discrete. In the present study discrete

* Corresponding author. E-mail: jszilagy@unlinfo.unl.edu

orthonormal wavelet expansions are applied to turbulence measurements in the atmospheric surface layer to identify the principal time scales of the coherent structures. As suggested by Yamada and Ohkitani[45], orthonormal wavelet transforms may be preferable since the orthogonality minimizes the number of wavelet coefficients and suppresses undesired relations between the coefficients.

For a discrete one-dimensional signal $f(j)$, discrete orthonormal wavelet coefficients are given by,

$$w^{(m)}[i] = \sum_{j=1}^{N} g^{(m)}[i - 2^m j] f[j], \tag{1}$$

where $w^{(m)}[i]$ is the wavelet coefficient at location i and scale m, and N is the total number of data points, which must be an integer power of two. The variable $g^{(m)}(i)$ is the dilated version of the discrete orthonormal basis function $g^{(0)}$ such that[6,8,28,29]

$$g^{(m)}[i] = 2^{-m/2} g^{(0)}\left[\frac{i}{2^m}\right]. \tag{2}$$

Note that in this arrangement, at scale index $m = 1$ there are $N/2$ wavelet coefficients, at scale index $m = 2$ there are $N/4$ coefficients, and so on, up to the single coefficient at scale index $m = M$, where $M = \log_2 N$. The original signal $f(j)$ can be reconstructed from its wavelet coefficients using

$$f(j) = \sum_{m=1}^{M} \sum_{i=1}^{N} w^{(m)}[i] g^{(m)}[i - 2^m j]. \tag{3}$$

In this paper three anti-symmetric (Daubechies-4, Daubechies-6, Daubechies-8) and three near-symmetric (Symlet-8, Symlet-12 and Symlet-16) basis functions (wavelets) are employed. The number in the name of the wavelet refers to the number of coefficients necessary to define the specific wavelet. This is done in order to study the effect of the choice of basis function on the analysis. Note that entirely symmetric orthonormal wavelets do not exist[9]. Consequently we applied the least anti-symmetric basis functions available[9].

Coherent structures or organized events in atmospheric time series are typically obscured by the superimposed incoherent part of the signal[19]. Wavelet decomposition allows us to separate the scales while maintaining the temporal reference. Regions of the time-scale half plane with high magnitudes of the squared wavelet coefficients correspond to strongly developed organized events at the given scale and time. As an example, the wavelet decomposition of a velocity signal measured in the lower atmosphere is presented in Fig. 1. Note that, near the time 260 s, and scale 128 s a strong coherent structure in the velocity signal is indicated by high values of the squared wavelet coefficients. The square of each wavelet coefficient, when scaled appropriately, is proportional to the contribution of the actual structure at time i and scale m to the variance of the measured signal. This is so because the following holds

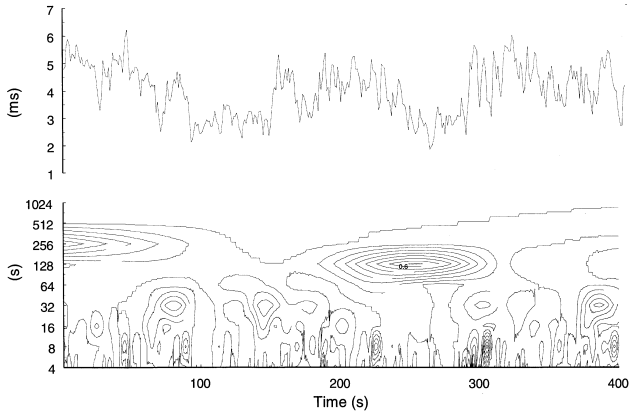

Fig. 1. A sample 1s block averaged longitudinal velocity time series and its discrete orthonormal wavelet transform with contours of the squared wavelet coefficients. The transformation was based on Newland's [35] algorithm.

(Parseval's identity) for the scaled wavelet coefficients $(\hat{w}^{(m)}(i))$

$$\sum_{j=1}^{N} f[j]^2 = \sum_{m=1}^{M} \sum_{i=1}^{2^{M-m}} (\hat{w}^{(m)}[i])^2, \tag{4}$$

where $\hat{w}^{(m)}(i)$ is equal to $2^{m/2} w^{(m)}(i)$.

Most methods proposed to identify coherent structure properties have subjective components[2,3,5,14,20,27,36,37,39,40]. For example, an arbitrary threshold value is set for the wavelet coefficients when selecting organized events, or the size of a certain window employed in the analysis must be specified. The result of the analysis, therefore, may depend on arbitrarily defined parameters that do not translate from one experimental site to the next.

In this study an objective, so-called global, method is proposed for calculating the principal duration time of coherent structures based upon discrete orthonormal basis functions. When applying the technique, the principal time scale is defined to be twice the scale in the time-scale half plane where the difference between the normalized (i.e. sum of the squared wavelet coefficients at the given scale divided by the sum of the variances of all scales) energy content of the measured data and that of a white noise process is maximum. The premise is that the larger the difference for each scale the more the data differ from a white noise process at those scales and consequently, the more intense is the role of the coherent structures at the corresponding scales.

The calculated principal time scales are compared with the results of a local technique proposed by Donoho and Johnstone[10,11] for signal de-noising. There only those wavelet coefficients are kept for the energy content calculation of different scales that are larger in magnitude than a certain universal threshold value. Since the low-magnitude wavelet coefficients, which are supposed to represent disorganized, random motion (i.e. noise) of the flow are discarded (set equal to zero), the remaining

wavelet coefficients are implied to be connected to the organized events. The principal time scale in this case is selected as twice the scale at which the normalized variances (sum of the thresholded squared wavelet coefficients) display a maximum.

2 DATA COLLECTION

Atmospheric surface layer measurements were carried out at the University of California, Davis, Campbell Tract Research Facility over a bare soil field (24 June, 1994 from 9:20 am to 3:00 pm) and over a bean crop field (29 August, 1994 from 9:20 am to 1:40 pm). The bare soil field had an average momentum roughness height (z_0) of 2 mm, while the bean field had an average momentum roughness height of 30 mm at the time of measurement. The vertical component of the wind velocity was recorded at 21 Hz by an ultrasonic anemometer located at 1.5 m above the soil surface and written into files of 20 min each.

The analysis is based on a total of 17 twenty-minute files for the bare soil and 13 for the bean field. Throughout the measurement periods unstable atmospheric stratification conditions prevailed.

Prior to analysis, the 21 Hz measurements were block averaged to 1 Hz, since the principal time scales of the coherent structures are expected to be at least an order of magnitude greater than 1 second[19,36]. As a result, the original 20 min data sets were reduced to 1024 ($=2^{10}$) data points.

3 ALGORITHMS

3.1 Proposed global method

The more distinct a turbulent structure is the higher will be the value of the squared wavelet coefficient at the corresponding location and scale[33]. Consequently, it is possible to estimate the relative contribution of the different coherent structure scales to the total variance of the signal using

$$p_m(d=2^{m+1}) = \frac{\sum_{i=1}^{2^{M-m}} (\hat{w}^{(m)}[i])^2}{\sum_{j=1}^{M}\sum_{k=1}^{2^{M-j}} (\hat{w}^{(j)}[k])^2} \quad m=1,\ldots,M, \tag{5}$$

where p_m is the portion of the total variance of the signal (see (4)) that can be attributed to structures with duration time d equal to 2^{m+1} (s). Note that the structure duration time d is defined as twice the actual wavelet scale after Lu and Fitzjarrald[27], who argue that the wavelet scale is comparable to the time period of updrafts for each coherent structure. The smallest structure detectable in this study has a duration of 4 s, since the Nyquist frequency for the block averaged data is 0.5 Hz.

As one might expect, the p_m values ($m=1,..M$) range between zero and one, and sum to unity.

If the data represent a white noise (wn) process, the expectation of the p_m values can be expressed as

$$\begin{aligned}
&\langle p_m^{\mathrm{wn}}(d=2^{m+1})\rangle \\
&= \frac{\sum_{i=1}^{2^{M-m}} \langle (\hat{w}^{(m)}[i])^2\rangle}{\sum_{j=1}^{M}\sum_{k=1}^{2^{M-j}} \langle (\hat{w}^{(j)}[k])^2\rangle} \\
&= \frac{\sum_{i=1}^{2^{M-m}} \mathrm{const}}{\sum_{j=1}^{M}\sum_{k=1}^{2^{M-j}} \mathrm{const}} = \frac{2^{-m}}{\sum_{j=1}^{M} 2^{-j}} \\
&= \frac{2^{M-m}}{2^M-1}, \quad m=1\ldots M,
\end{aligned} \tag{6}$$

where we make use of the white noise property that the expected value of the squared and properly scaled wavelet coefficients is constant for each scale.

The maximum of the p_m values for (5) does not signify the predominance of the different structure durations, since even in the case of a white noise process the expectation of the p_m values are not evenly distributed across the scales (see Fig. 2). This is because the number of wavelet coefficients to be summed for each scale decreases exponentially with increasing m, resulting in the general exponential type decay of the p_m^{wn} values displayed in Fig. 2. In order to obtain a useful estimate of the relative importance of the different coherent structure scales, the p_m^{wn} values for each scale of the white noise process have to be subtracted from the same p_m values of the turbulent measurements. This way, the remaining part of the p_m values are not the result of disorganized, random motions. The greater this difference for a given scale, the more organized is the measured signal at that particular scale. In this way, the scale with the largest positive value in the difference ($p_m - p_m^{\mathrm{wn}}$) corresponds to (one-half) the principal time scale of the coherent structures in the turbulent flow. In Fig. 3(a), (b) these differences are presented applying anti- and near-symmetric wavelets for the vertical component of atmospheric flow measurements over bare soil and a bean field, respec-

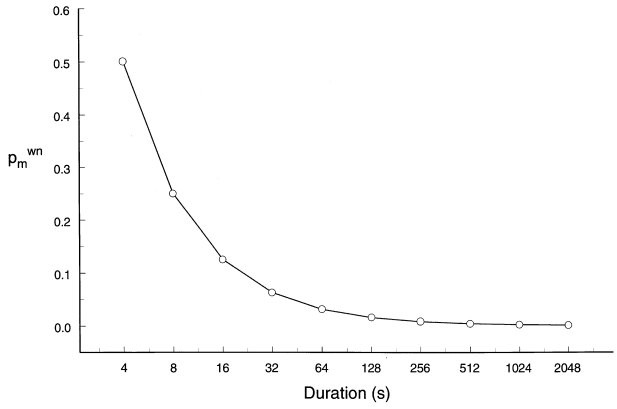

Fig. 2. Normalized energies (p_m) of the wavelet scales. White noise process.

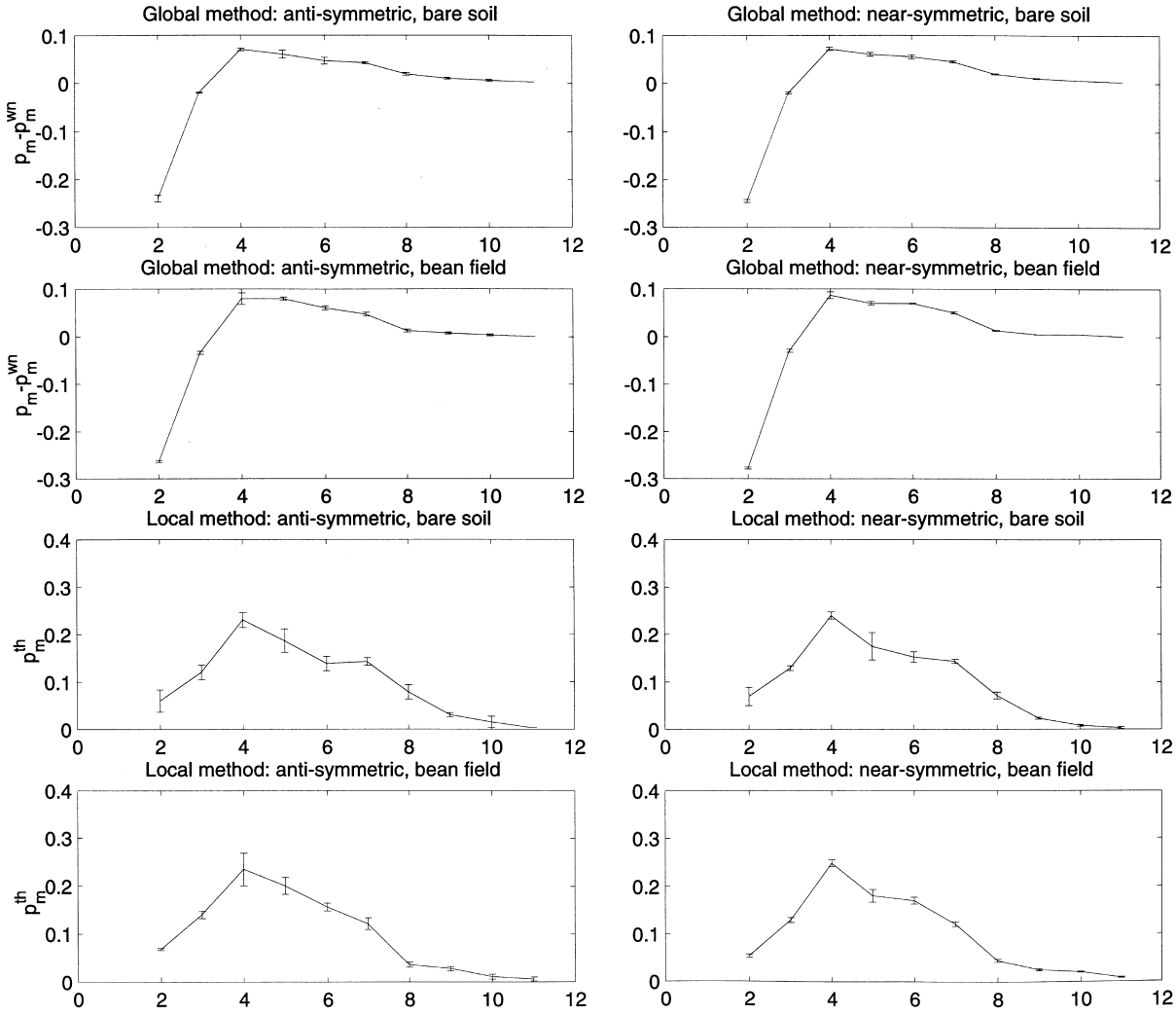

Fig. 3. Normalized and corrected variances ($p_m - p_m^{\mathrm{wn}}$) of the wavelet scales (mean and standard error) by the global method using anti- and near-symmetric wavelets. Also normalized thresholded variances (p_m^{th}) of the wavelet scales (mean and standard error) by the local method using anti- and near-symmetric wavelets. The exponents of 2 are shown on the horizontal axes.

tively. The peak in each graph marks the principal time scale of the coherent structures.

3.2 Donoho and Johnstone's local method

Donoho and Johnstone[10,11] and Donoho[12] proposed a universal thresholding value for noise separation of multidimensional signals when wavelet transforms are applied. The underlying idea is that the noise of the signal is represented by mostly low-magnitude coefficients in the time-scale half plane. Using only the high-magnitude wavelet coefficients in the inverse transform, the original signal can be reconstructed with dramatic reduction in the noise level[11]. We assume that the same approach can be used for the detection of coherent structures in a turbulent flow, if the disorganized part of the flow is considered as a noise. Donoho and Johnstone[10,11] showed that choosing a threshold value, th as

$$\mathrm{th} = \sigma(2\ln(K))^{1/2}, \tag{7}$$

where K is the number of wavelet coefficients at the finest scale ($=512$ in our case), and σ is the estimated median absolute deviation (divided by 0.6745) of the wavelet coefficients at the same scale, provides near-optimal performance in noise reduction if the noise is white. After comparing the magnitude of each wavelet coefficient with the value of th and setting all coefficients equal to zero that are smaller in magnitude than th, (5) was employed. The resulting p_m^{th} values for the vertical velocities recorded over bare soil and the bean field are displayed in Fig. 3(c), (d).

Comparing Fig. 3(a), (b) with Fig. 3(c), (d), it can be seen that the two methods (i.e. global and local) resulted in a principal time scale of 16 s for the vertical velocities over both fields. Fig. 3(c), (d) displays wider error bars than Fig. 3(a), (b) due to the smaller number of the wavelet coefficients employed in the local method.

4 DISCUSSION

Based upon the above described methods of identifying coherent structures, the analysis of vertical velocities over bare soil and a bean field revealed the following:

(1) The principal time scale of coherent structures for the vertical velocities was found to be around 16 s over both fields (bare soil and bean). This is in agreement with Qiu *et al.*,[36] who applied pseudo-wavelet analysis for coherent structure identification for flow over a maize field under similar meteorological conditions. They found the same principal time scale for the vertical velocities (about 15 s) at the top of the canopy.

(2) The resulting principal time scales were only slightly dependent (due to minor scatter of points in Fig. 3(a)–(d)) on the choice of the basis function within the same type (i.e. near-symmetric or anti-symmetric). The two methods (i.e. global. vs. local) gave identical results with the global method expressing less scatter due to the larger number of wavelet coefficients employed in the technique. Since Hagelberg and Gamage[22] demonstrated that anti-symmetric wavelets are more sensitive in detecting zones of sharp transitions connected to coherent structures, the use of anti-symmetric basis functions is perhaps better suited to the present effort.

In summary, the application of the global method, with the use of anti-symmetric wavelets, is recommended for coherent structure principal time scale calculations because the technique retains all the wavelet coefficients fully representing the original signal. The principal time scale in the method is defined as twice the scale where the associated energy (calculated via the squared wavelet coefficients) has a maximum above a reference (white noise) energy level. In contrast, thresholding methods discard squared wavelet coefficients with values smaller than a certain threshold value before calculating energies distributed over scales, with the inherent assumption that the remaining squared wavelet coefficients represent the energy associated only with the structure containing part of the turbulence signal. An ambiguity remains as how to choose the right threshold value, since various authors propose different values. Donoho and Johnstone[10,11] and Donoho[12] derived an algorithm to select a threshold value for near-optimal noise reduction in the presence of white noise. The application of the so derived threshold value was presented in the local method. However, since the non-structure component of atmospheric turbulent signals cannot be considered to be pure white noise due to the significant slope of the corresponding non-structure energy spectrum[21,22,42], the near-optimal behavior of the local method in these cases might not be guaranteed.

ACKNOWLEDGEMENTS

The authors are grateful to the three anonymous reviewers for their valuable comments on a previous version of the manuscript.

REFERENCES

1. Antonia, R. A., Friehe, C. A. & van Atta, C. W. Temperature ramps in the atmospheric surface layer. *J. Atmos. Sci.*, 1979, **36,** 99–108.
2. Antonia, R. A., Rajagopalan, S. & Chambers, A. J. Conditional sampling of turbulence in the atmospheric surface layer. *J. Clim. Appl. Meteorol.*, 1983, **22,** 69–78.
3. Baldocchi, D. D. & Meyers, T. P. Turbulence structure in a deciduous forest. *Boundary-Layer Meteor.*, 1988, **43,** 345–365.
4. Bergstrom, H. & Hogstrom, U. Turbulent exchange above a pine forest. II. Organized structures. *Boundary-Layer Meteor.*, 1989, **49,** 231–263.
5. Blackwelder, R. F. & Kaplan, R. E. On the bursting phenomenon near the wall in bounded turbulent shear flows. *J. Fluid Mech.*, 1976, **76,** 89–112.
6. Chui, C. K. *An Introduction to Wavelets*. Academic Press, Boston, 1992.
7. Collineau, S. & Brunet, Y. Detection of turbulent coherent motions in a forest canopy. Part II: Time scales and conditional averages. *Boundary-Layer Meteor.* 1993, **66,** 49–73.
8. Daubechies, I. Orthonormal bases of compactly supported wavelets. *Comm. Pure Appl. Math.*, 1988, **41,** 909–996.
9. Daubechies, I. *Ten Lectures on Wavelets*. Society for Industrial and Applied Mathematics, Philadelphia, PA, 1992.
10. Donoho, D. L. & Johnstone, I. M. Bank of wavelet-related technical reports at *playfair.stanford.edu*, 1992, 1993.
11. Donoho, D. L. & Johnstone, I. M. Ideal spatial adaptation by wavelet shrinkage. *Biometrika*, 1994, **81,** 425–455.
12. Donoho, D. L. De-Noising by soft-thresholding. *IEEE Trans. Inform. Theory*, 1995, **41,** 613–627.
13. Farge, M. Wavelet transforms and their applications to turbulence. *Ann. Rev. Fluid Mech.,* 1992, **24,** 395–457.
14. Finnigan, J. J. Turbulence in waving wheat. II: Structure of momentum transfer. *Boundary-Layer Meteor.*, 1979, **16,** 213–236.
15. Gamage, N. & Hagelberg, C. Detection and analysis of microfronts and associated coherent events using localized transforms. *J. Atmos. Sci.*, 1993, **50,** 750–756.
16. Gao, W., Shaw, R. H., & Paw U, K. T. Observation of organized structure in turbulent flow within and above a forest canopy. *Boundary-Layer Meteorol.*, 1989, **47,** 349–377.
17. Gao W., Shaw, R. H. & Paw U, K. T. Characteristics of large eddy transport between the lower atmosphere and a deciduous forest. *Proceedings of the 20th Conference on Agricultural and Forest Meteor., Salt Lake City, UT*, Amer. Meteor. Soc., 1991, 155–157.
18. Gao, W. & Shaw, R. H. Conditional analysis of temperature and humidity microfronts and ejection/sweep mo-

tions within and above a deciduous forest. *Boundary-Layer Meteor.*, 1992, **59,** 35–57.
19. Gao, W. & Li, B. L. Wavelet analysis of coherent structures at the atmosphere-forest interface. *J. Applied Meteorol.*, 1993, **32,** 1717–1725.
20. Grass, A. J. Structural features of turbulent flow over smooth and rough boundaries. *J. Fluid Mech.*, 1971, **50,** 233–255.
21. Hagelberg, C. R. & Gamage, N. K. K. Structure-preserving wavelet decompositions of intermittent turbulence. *Boundary-Layer Meteor.*, 1994a, **70,** 217–246.
22. Hagelberg, C. R. & Gamage, N. K. K., Application of structure preserving wavelet decompositions to intermittent turbulence: A case study, in: E. Foufoula-Georgiou & P. Kumar (Eds.), *Wavelet Transforms in Geophysics, Vol. IX in Wavelet Analysis & its Applications*, C. Chui, series editor, Academic Press, New York, 1994b.
23. Katul, G. G. & Parlange, M. B. On the active role of temperature in surface-layer turbulence. *J. Atm. Sci.*, 1994, **51,** 2181–2195.
24. Katul, G. G., Parlange, M. B. & Chu, C. R. Intermittency, local isotropy, and non-Gaussian statistics in atmospheric surface layer turbulence. *Phys. Fluids*, 1994, **6(7)**, 2480–2492.
25. Katul, G. G. & Vidakovic, B. The partitioning of attached & detached eddy motion in the atmospheric surface layer using Lorentz wavelet filtering. *Boundary-Layer Meteor.*, 1996, **77,** 153–172.
26. Liandrat, J. & Moret-Bailly, F. The wavelet transform: Some applications to fluid dynamics and turbulence. *Eur. J. Mech.*, 1990, **B9,** 1–19.
27. Lu, C. & Fitzjarrald, D. R. Seasonal & diurnal variations of coherent structures over a deciduous forest. *Boundary-Layer Meteorol.*, 1993, **69,** 43–69.
28. Mallat, S. A theory for multiresolution signal decomposition: The wavelet representation. *IEEE Trans. Pattern Analysis and Machine Intelligence*, 1989a, **11,** 674–693.
29. Mallat, S. Multiresolution approximations and wavelet orthonormal bases of $L^2(R)$. *Trans. Amer. Math. Soc.*, 1989b, **315,** 69–87.
30. Mahrt, L. Eddy asymmetry in the shear heated boundary layer. *J. Atmos. Sci.*, 1991, **48,** 472–492.
31. Mahrt, L. & Gibson, W. Flux decomposition into coherent structures. *Boundary-Layer Meteor.*, 1992, **60,** 142–168.
32. Mahrt, L. & Howell, J. F. The influence of coherent structures and microfronts on scaling laws using global and local transforms. *J. Fluid Mech.*, 1994, **260,** 247–270.
33. Meneveau, C. Analysis of turbulence in the orthonormal wavelet representation. *J. Fluid. Mech.*, 1991a, **232,** 469–520.
34. Meneveau, C. Dual spectra and mixed energy cascade of turbulence in the wavelet representation. *Phys. Rev. Lett.*, 1991b, **11,** 1450–1453.
35. Newland, D. E. *Random Vibrations, Spectral and Wavelet Analysis.* Longman Scientific and Technical, New York, 1993.
36. Qiu, J., Paw U, K. T. & Shaw, R. H. Pseudo-wavelet analysis of turbulence patterns in three vegetation layers. *Boundary-Layer Meteorol.*, 1995, **72,** 177–204.
37. Raupach, M. R. Conditional statistics of Reynolds stress in rough wall and smooth wall turbulent boundary layer. *J. Fluid Mech.*, 1981, **108,** 363–382.
38. Raupach, M. R., Finnigan, J. J. & Brunet, Y. Coherent eddies in vegetation canopies. *Proceedings of the Fourth Australasian Conference on Heat and Mass Transfer*, Christchurch, New Zealand, 9-12 May, 1989, 75–90.
39. Schols, J. L. J. The detection and measurements of turbulent structures in the atmospheric Surface Layer. *Boundary-Layer Meteorol.*, 1994, **69,** 39–58.
40. Shaw, R. H., Paw U, K. T. & Gao, W. Detection of temperature ramps and flow structures at a deciduous forest site. *Agric. For. Meteorol.*, 1989, **47,** 123–138.
41. Sullivan, P., Day, M. & Pollard, A. Enhanced VITA technique for turbulent structure identification. *Exp. Fluids*, 1994, **18,** 10–16.
42. Szilagyi, J., Katul, G. G., Parlange, M. B., Albertson, J. D. & Cahill, A. T. The local effect of intermittency on the inertial subrange energy spectrum of the atmospheric surface layer, *Boundary Layer Meteorol.*, 1996, **79,** 35–50.
43. Turner, B. J., Leclerc, M. Y., Gauthier, M., Moore, K. E. & Fitzjarrald, D. R. Identification of turbulence structures above a forest canopy using a wavelet transform. *J. Geophys. Res.*, 1994, **99 D1** 1919–1926.
44. Wilczak, J. M. Large-scale eddies in the unstably stratified atmospheric surface layer. Part I: Velocity and temperature structures. *J. Atmos. Sci.*, 1984, **41,** 3537–3550.
45. Yamada, M. & Ohkitani, K. Orthonormal expansion and its application to turbulence. *Prog. Theor. Phys.: Progress Lett.*, 1990, **86,** 819–823.